2020 17th International Conference on Electrical Engineering, Computing Science and Automatic Control (CCE)
Mexico City, Mexico. November 11-13, 2020

Quadrotor novel model for trajectory tracking using neural sliding modes in discrete-time

Julio A. Flórez[1], Luz A. Vega[2], Edgar N. Sanchez[1] and Alexander G. Loukianov.[1]
[1]CINVESTAV-IPN, Electrical Engineering Department
Av del Bosque 1145 El Bajío, 45019 Zapopan, Jalisco, México
{jaflorez,sanchez,louk}@gdl.cinvestav.mx
[2]Industrial University of Santander, School of Mechanical Engineering
Cra 27 Calle 9, 680003, Bucaramanga, Santander, Colombia
luz.vega1@correo.uis.edu.co

***Abstract*— This paper addresses the solution of a trajectory tracking a quadrotor considering plant parameter variations, proposing a novel model. First a novel model of the quadrotor is developed, considering different phenomena such as: blade flapping and drag force. By means of a discrete-time Recurrent High-Order Neural Network trained with an extended Kalman filter algorithm, neural model is identified for the quadrotor. Then, it is transformed using the block control technique in order to design a sliding surface, which depends on the tracking errors. Finally, a non-switching discrete-time sliding mode control is applied to ensure the aforementioned sliding surface be attractive. The effectiveness of the proposed based on simulations.**

***Index Terms*— Quadrotor, modelling, aerodynamic effects, recurrent neural network, block control, discrete-time sliding modes.**

I. INTRODUCTION

Based on fundamentals of vector dynamics, aerodynamics, and fluid mechanics, the present paper proposes an alternative quadrotor model, which it able to do *pitch* and *roll* maneuvers with inclination angles close to $\pm 45\,[^\circ]$ in practice, with a mathematical restriction at $\pm 90\,[^\circ]$. In addition, it allows to change the quadrotor orientation with a restriction of $\pm 360\,[^\circ]$ to avoid confusion between the reference frames [1]. This model considers some environmental effects which are not normally taken into account, such as drag force, and wind turbulence and which can significantly affect the dynamical behavior [2], [3]. Trajectory tracking of the quadrotor is addressed by proposing a recurrent high-order neural network (RHONN) identifier, trained on-line using an extended Kalman filter, which allows obtain good performance even in presence of disturbance caused for impressions in the parameters associated with the mathematical model or operational environment [4], [5], [6]. Based on this neural identifier, the quadrotor is represented in the block control form, applying on its last block a non-switching discrete-time sliding mode technique, which provides a smooth behavior when the motion is on the sliding manifold. It is worth noting, that robustness is ensured by combination of the Neural Network identifier and the discrete SM control; although continuous SM control on its own is robust to matched perturbations, robustness is preserved for discrete SM control [7], [8], [9].

978-1-7281-8987-1/20/$31.00

II. QUADROTOR MODEL

The quadrotor model is obtained from the vectorial dynamics, considering translation and rotation through two frames of reference: an inertial frame $\mathcal{I}$ located in the center earth with cartesian coordinates $(x, y, z)_{\mathcal{I}}$ and a body one $\mathcal{B}$ located in the mass center of the quadrotor with cartesian coordinates $(X, Y, Z)_{\mathcal{B}}$. The orientation the quadrotor body frame relative to the fixed inertial frame follows the 3-2-1 rotation sequence of the Euler angles $(\psi, \theta, \varphi)_{\mathcal{B}}^{\mathcal{I}}$, where ψ is *yaw* rotation about the inertial 3-axis, θ is *pitch* rotation about the intermediate frame 2-axis, and φ is *roll* rotation. Thus the transformation matrix between the inertial frame $\mathcal{I}$ and the body frame $\mathcal{B}$, which relates the body reference frame to the inertial reference frame is given by

$$ {}^{\mathcal{I}}R^{\mathcal{B}} = \begin{bmatrix} \mathrm{c}\theta\mathrm{c}\psi & \mathrm{s}\varphi\mathrm{s}\theta\mathrm{c}\psi - \mathrm{c}\varphi\mathrm{s}\psi & \mathrm{c}\varphi\mathrm{s}\theta\mathrm{c}\psi + \mathrm{s}\varphi\mathrm{s}\psi \\ \mathrm{c}\theta\mathrm{s}\psi & \mathrm{s}\varphi\mathrm{s}\theta\mathrm{s}\psi + \mathrm{c}\varphi\mathrm{c}\psi & \mathrm{c}\varphi\mathrm{s}\theta\mathrm{s}\psi - \mathrm{s}\varphi\mathrm{c}\psi \\ -\mathrm{s}\theta & \mathrm{s}\varphi\mathrm{c}\theta & \mathrm{c}\varphi\mathrm{c}\theta \end{bmatrix}, $$

where $\sin\alpha = s\alpha$ and $\cos\alpha = c\alpha$.

The quadrotor motion is displayed in Fig. 1, where imbalance between thrusts $\mathbf{T}_1$ and $\mathbf{T}_2$ produces an attack angle θ, which generates a movement in the direction of $\mathbf{b}_1$, while imbalance between thrusts $\mathbf{T}_3$ and $\mathbf{T}_4$ do the same for obtain movement in $\mathbf{b}_2$ through an angle φ. Additionally, when it is considered the spinning sense of the rotors, where the propellers 1-2 rotate in clockwise while 3-4 do the same counter-clockwise, imbalance between the total thrust in clockwise and counter-clockwise produces an angle of rotation ψ around of axis $\mathbf{b}_3$ which change the orientation of the quadrotor. Here $\mathbf{e}_i, \mathbf{b}_i$, $\forall i = 1, 2, 3$, correspond to unit vectors of the reference frames $\mathcal{I}$ and $\mathcal{B}$, respectively [1].

Two effects are in the model. The first one named as *blade flapping*, which introduces both moments in the rotors for the pitch and roll; it can be seen as a deflection in the thrust vector perpendicular to the blade rotation plane; The second one corresponds to the *drag force*, which is always present when an object moves through a fluid.

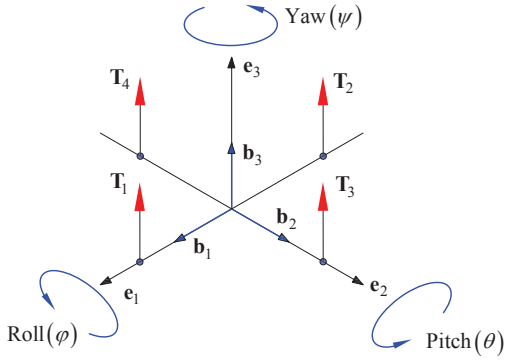

Fig. 1: Quadrotor rotation with respect to inertial frame

A. Blade Flapping

Assuming that the thrust of the λ-*th* rotor $\mathbf{T}_\lambda = T_\lambda \mathbf{b}_3$ is affected for the incident air-relative velocity given by

$$\mathbf{V}_{rel,\lambda} = u_\lambda \mathbf{b}_1 + v_\lambda \mathbf{b}_2 + w_\lambda \mathbf{b}_3, \tag{1}$$

blade flapping appears when the components $\mathbf{b}_1$ and $\mathbf{b}_2$ of (1), it hit the propeller blade at a flap angle α_λ, such that is shown in Fig. 2. Thus the thrust of the λ-*th* rotor is expressed as

$$\mathbf{T}_\lambda = T_\lambda \left(\delta_{u,\lambda} \sin(\alpha_\lambda)\mathbf{b}_1 + \delta_{v,\lambda} \sin(\alpha_\lambda)\mathbf{b}_2 + \cos(\alpha_\lambda)\mathbf{b}_3\right),$$

where $\delta_{u,\lambda}$ and $\delta_{v,\lambda}$ are bounded disturbances that affect the total thrust of the rotor proportional to the incident air-relative velocity [2].

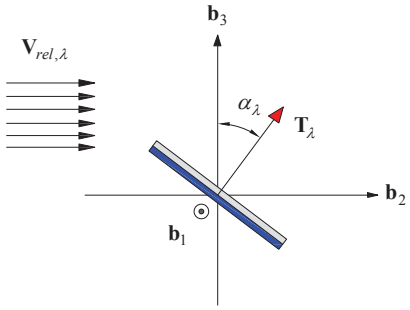

Fig. 2: Blade flapping

B. Drag Force

In fluid dynamics, the drag force $\mathbf{D}$ acts in the opposite sense to the advance of the vehicle, such as is shown in Figure 3, where $\mathbf{T}_1, ..., \mathbf{T}_4$ are the thrusts of the rotors, g is the gravity acceleration, m_G the total mass of quadrotor, and $\mathbf{V}_{G/0}$ is the translation velocity of the quadrotor. Assuming that the drag force acts at the mass center, such that, it no causes moments upon the quadrotor, the drag force is given by

$$\mathbf{D} = D_1\mathbf{b}_1 + D_2\mathbf{b}_2 + D_3\mathbf{b}_3 = C_d \left\|\mathbf{V}_G\right\|^2 \hat{\mathbf{V}}_G \tag{2}$$

where C_d is a drag coefficient, and $\hat{\mathbf{V}}_G$ is the unit vector of the relative velocity at the mass center is defined as

$$\mathbf{V}_G = u_G\mathbf{b}_1 + v_G\mathbf{b}_2 + w_G\mathbf{b}_3, \tag{3}$$

such that, for a wind velocity in the body reference frame $\mathbf{V}_w = u_w\mathbf{b}_1 + v_w\mathbf{b}_2 + w_w\mathbf{b}_3$, the component of (3) corresponds to $u_G = u_w - u, v_G = v_w - v, w_G = w_w - w$, where $\{v, u, w\}$ are velocity magnitude in body axes $\{\mathbf{b}_1, \mathbf{b}_2, \mathbf{b}_3\}$, respectively [3].

On the other hand, defining the state vector in continuous-time as $\mathbf{x} = [\varphi, \theta, \psi, p, q, r, x, y, z, u, v, w]^T$, the inputs of control as $\mathbf{u} = [u_1, u_2, u_3, u_4]^T$, the outputs which describe the displacement of the quadrotor as $\bar{\mathbf{y}} = [x, y, z, \psi]^T$, and omitting the disturbances caused by the blade flapping, and doing $\alpha_\lambda = 0$, without loss of generality, the quadrotor model considered for the synthesis of the controllers can be represented in space state as

$$\begin{aligned}
\dot{x}_1 &= x_4 + x_5 \sin x_1 \tan x_2 + x_6 \cos x_1 \tan x_2 \\
\dot{x}_2 &= x_5 \cos x_1 - x_6 \sin x_1 \\
\dot{x}_3 &= x_5 \frac{\sin x_1}{\cos x_2} + x_6 \frac{\cos x_1}{\cos x_2} \\
\dot{x}_4 &= -\frac{(I_3 - I_2)}{I_1} x_5 x_6 + \frac{u_1}{I_1} \\
\dot{x}_5 &= -\frac{(I_1 - I_3)}{I_2} x_4 x_6 + \frac{u_2}{I_2} \\
\dot{x}_6 &= -\frac{(I_2 - I_1)}{I_3} x_4 x_5 + \frac{u_3}{I_3} \\
\dot{x}_7 &= x_{10} \cos x_2 \cos x_3 + x_{11} \left(\sin x_1 \sin x_2 \cos x_3 \right. \\
&\quad \left. - \cos x_1 \sin x_3\right) + x_{12} \left(\cos x_1 \sin x_2 \cos x_3 \right. \\
&\quad \left. - \sin x_1 \sin x_3\right) \\
\dot{x}_8 &= x_{10} \cos x_2 \sin x_3 + x_{11} \left(\sin x_1 \sin x_2 \sin x_3 \right. \\
&\quad \left. + \cos x_1 \cos x_3\right) + x_{12} \left(\cos x_1 \sin x_2 \sin x_3 \right. \\
&\quad \left. - \sin x_1 \cos x_3\right) \\
\dot{x}_9 &= -x_{10} \sin x_2 + x_{11} \sin x_1 \cos x_2 \\
&\quad + x_{12} \cos x_1 \cos x_2 \\
\dot{x}_{10} &= x_6 x_{11} - x_5 x_{12} + \frac{D_1}{m_G} + g \sin x_2 \\
\dot{x}_{11} &= x_4 x_{12} - x_6 x_{10} + \frac{D_2}{m_G} - g \sin x_1 \cos x_2 \\
\dot{x}_{12} &= x_5 x_{10} - x_4 x_{11} + \frac{D_3}{m_G} - g \cos x_1 \cos x_2 + \frac{u_4}{m_G}
\end{aligned} \tag{4}$$

with

$$\mathbf{u} = \begin{bmatrix} u_1 \\ u_2 \\ u_3 \\ u_4 \end{bmatrix} = \begin{bmatrix} L\left(T_3 - T_4\right) \\ L\left(T_2 - T_1\right) \\ \kappa_S\left(T_1 + T_2 - T_3 - T_4\right) \\ T_1 + T_2 + T_3 + T_4 \end{bmatrix}, \tag{5}$$

where κ_S is a constant that relates the applied thrust to the moment induced by spinning the rotor.

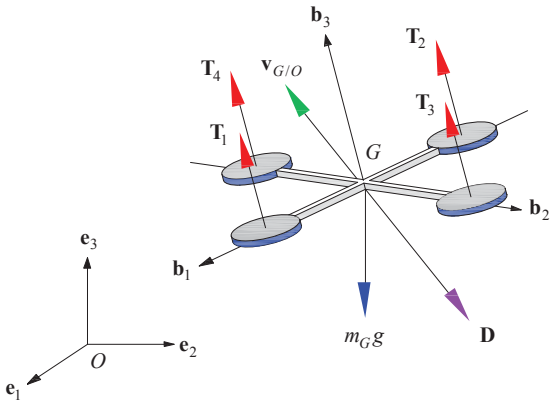

Fig. 3: Drag force

III. QUADROTOR NEURAL IDENTIFICATION AND SM CONTROL

A. Neural Identifier

Using Euler's discretization with a sampling time of T_s, from (4), a neural model for the quadrotor is proposed, based on a neural network representing the state- space innovations form model [4], [5], as follows

$$
\begin{aligned}
\hat{x}_{1,k+1} &= \Omega_{1,1,k} + \Omega_{1,2,k}x_{4,k} + \Omega_{1,3,k}x_{5,k} + \Omega_{1,4,k}x_{6,k}\\
\hat{x}_{2,k+1} &= \Omega_{2,1,k} + \Omega_{2,2,k}x_{5,k} + \Omega_{2,3,k}x_{6,k}\\
\hat{x}_{3,k+1} &= \Omega_{3,1,k} + \Omega_{3,2,k}x_{5,k} + \Omega_{3,3,k}x_{6,k}\\
\hat{x}_{4,k+1} &= w_{4,1,k}z_{1,k} + w_{4,2,k}z_{2,k} + \Omega_{4,3,k}u_{1,k}\\
\hat{x}_{5,k+1} &= w_{5,1,k}z_{3,k} + w_{5,2,k}z_{4,k} + \Omega_{5,3,k}u_{2,k}\\
\hat{x}_{6,k+1} &= w_{6,1,k}z_{5,k} + w_{6,2,k}z_{6,k} + \Omega_{6,3,k}u_{3,k}\\
\hat{x}_{7,k+1} &= \Omega_{7,1,k} + \Omega_{7,2,k}x_{10,k} + (\Omega_{7,3,k} + \Omega_{7,4,k})\, x_{11,k}\\
&\quad + (\Omega_{7,5,k} + \Omega_{7,6,k})\, x_{12,k}\\
\hat{x}_{8,k+1} &= \Omega_{8,1,k} + \Omega_{8,2,k}x_{10,k} + (\Omega_{8,3,k} + \Omega_{8,4,k})\, x_{11,k}\\
&\quad + (\Omega_{8,5,k} + \Omega_{8,6,k})\, x_{12,k} \qquad (6)\\
\hat{x}_{9,k+1} &= \Omega_{9,1,k} + \Omega_{9,2,k}x_{10,k} + \Omega_{9,3,k}x_{11,k} + \Omega_{9,4,k}x_{12,k}\\
\hat{x}_{10,k+1} &= \Omega_{10,1,k} + \Omega_{10,2,k} + \Omega_{10,3,k} + \Omega_{10,4,k}\\
&\quad + w_{10,5,k}z_{7,k}\\
\hat{x}_{11,k+1} &= \Omega_{11,1,k} + \Omega_{11,2,k} + \Omega_{11,3,k} + \Omega_{11,4,k}\\
&\quad + w_{11,5,k}z_{8,k}\\
\hat{x}_{12,k+1} &= \Omega_{12,1,k} + \Omega_{12,2,k} + \Omega_{12,3,k} + \Omega_{12,4,k}\\
&\quad + w_{12,5,k}z_{9,k} + \Omega_{12,6,k}u_{4,k}
\end{aligned}
$$

where $\{u_{1,k}, u_{2,k}, u_{3,k}, u_{4,k}\}$ are the system imputs, $z_{i,k}$ with $i = 1,\ldots,9$ are high-order terms, and $\{\Omega_{1,1,k},\ldots,\Omega_{12,6,k}\}$ are a set of calculated weights shown in the Table I, $\sin\alpha = s\alpha$, $\cos\alpha = c\alpha$ and $\tan\alpha = tg\alpha$. The terms $\hat{x}_{i,k}$, with $i = 1,\ldots,12$, are the estimated states of the quadrotor model (4).

B. Block Control

The control scheme presented in Fig. 4 contains the structure used for the on-line controller: the synaptic weights

TABLE I: Calculated weights

Weight	Value	Weight	Value
$\Omega_{1,1,k}$	$x_{1,k}$	$\Omega_{8,3,k}$	$T_s sx_{1,k} sx_{2,k} sx_{3,k}$
$\Omega_{1,2,k}$	T_s	$\Omega_{8,4,k}$	$T_s cx_{1,k} cx_{3,k}$
$\Omega_{1,3,k}$	$T_s sx_{1,k} tgx_{2,k}$	$\Omega_{8,5,k}$	$T_s cx_{1,k} sx_{2,k} sx_{3,k}$
$\Omega_{1,4,k}$	$T_s cx_{1,k} tgx_{2,k}$	$\Omega_{8,6,k}$	$-T_s sx_{1,k} cx_{3,k}$
$\Omega_{2,1,k}$	$x_{2,k}$	$\Omega_{9,1,k}$	$x_{9,k}$
$\Omega_{2,2,k}$	$T_s cx_{1,k}$	$\Omega_{9,2,k}$	$-T_s sx_{2,k}$
$\Omega_{2,3,k}$	$-T_s sx_{1,k}$	$\Omega_{9,3,k}$	$T_s sx_{1,k} sx_{2,k}$
$\Omega_{3,1,k}$	$x_{3,k}$	$\Omega_{9,4,k}$	$T_s cx_{1,k} cx_{2,k}$
$\Omega_{3,2,k}$	$T_s sx_{1,k}/cx_{2,k}$	$\Omega_{10,1,k}$	$x_{10,k}$
$\Omega_{3,3,k}$	$T_s cx_{1,k}/cx_{2,k}$	$\Omega_{10,2,k}$	$T_s x_{6,k} x_{11,k}$
$\Omega_{4,3,k}$	T_s/I_1	$\Omega_{10,3,k}$	$-T_s x_{5,k} x_{12,k}$
$\Omega_{5,3,k}$	T_s/I_2	$\Omega_{10,4,k}$	$T_s g\, sx_{2,k}$
$\Omega_{6,3,k}$	T_s/I_3	$\Omega_{11,1,k}$	$x_{11,k}$
$\Omega_{7,1,k}$	$x_{7,k}$	$\Omega_{11,2,k}$	$T_s x_{4,k} x_{12,k}$
$\Omega_{7,2,k}$	$T_s cx_{2,k} cx_{3,k}$	$\Omega_{11,3,k}$	$-T_s x_{6,k} x_{10,k}$
$\Omega_{7,3,k}$	$T_s sx_{1,k} sx_{2,k} cx_{3,k}$	$\Omega_{11,4,k}$	$-T_s g\, sx_{1,k} cx_{2,k}$
$\Omega_{7,4,k}$	$-T_s cx_{1,k} sx_{3,k}$	$\Omega_{12,1,k}$	$x_{12,k}$
$\Omega_{7,5,k}$	$T_s cx_{1,k} sx_{2,k} cx_{3,k}$	$\Omega_{12,2,k}$	$T_s x_{5,k} x_{10,k}$
$\Omega_{7,6,k}$	$T_s sx_{1,k} sx_{3,k}$	$\Omega_{12,3,k}$	$-T_s x_{4,k} x_{11,k}$
$\Omega_{8,1,k}$	$x_{8,k}$	$\Omega_{12,4,k}$	$-T_s g\, cx_{1,k} cx_{2,k}$
$\Omega_{8,2,k}$	$T_s cx_{2,k} sx_{3,k}$	$\Omega_{12,6,k}$	T_s/m_G

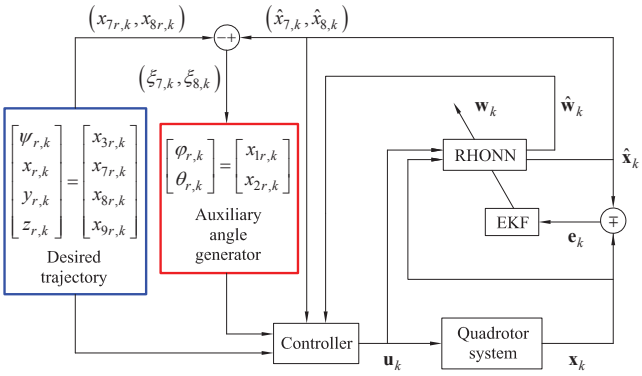

Fig. 4: Neural control scheme. The blue box corresponds to the desired trajectory while that the red ones calculates indirectly the angular references required for moving in the plane $\mathbf{e}_1 - \mathbf{e}_2$, based on the tracking errors in the states $\hat{x}_{7,k}$ and $\hat{x}_{8,k}$.

are adapted at each k instant by an extended Kalman filter (EKF), using the estimation error $\mathbf{e}_k$ of the system states to obtain optimal weights. Furthermore, it can be seen that the rotation references $x_{1r,k}$ and $x_{2r,k}$ are generated implicitly through the translation error of the states $\hat{x}_{8,k}$ and $\hat{x}_{7,k}$, respectively. For this plant, the block control structure corresponds to two individual block control related each to other, where the stability of the translational dynamic depends on the stability of the rotational dynamic. Fig. 5, it can be seen as a hierarchical control with rotational dynamics at the top, whose states directly influence the behaviour of the translational dynamics

Rotational blocks: From (6) the variables of the first rotational block (Block A) are defined as

$$
\mathbf{x}_{1,k} = \begin{bmatrix} \hat{x}_{1,k} - x_{1r,k} \\ \hat{x}_{2,k} - x_{2r,k} \\ \hat{x}_{3,k} - x_{3r,k} \end{bmatrix}, \quad \mathbf{x}_{2,k} = \begin{bmatrix} \hat{x}_{4,k} \\ \hat{x}_{5,k} \\ \hat{x}_{6,k} \end{bmatrix},
$$

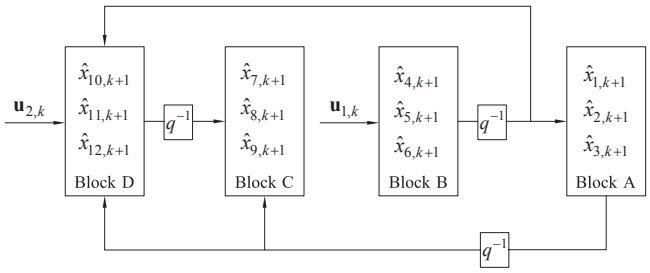

Fig. 5: Block control scheme. The blocks D and C correspond to the translational block control, while the blocks B and A to the rotational one.

so that the state estimation is expressed in the block control form as

$$\mathbf{x}_{1,k+1} = \mathbf{f}_{1,k}(\mathbf{x}_{1,k}, \hat{\mathbf{w}}_k) + \mathbf{B}_{1,k}\mathbf{x}_{2,k}, \tag{7}$$

$$\mathbf{x}_{2,k+1} = \mathbf{f}_{2,k}(\mathbf{x}_{2,k}, \hat{\mathbf{w}}_k) + \mathbf{B}_{2,k}\mathbf{u}_{1,k}, \tag{8}$$

with

$$\mathbf{f}_{1,k} = \begin{bmatrix} \Omega_{1,1,k} - x_{1r,k+1} \\ \Omega_{2,1,k} - x_{2r,k+1} \\ \Omega_{3,1,k} - x_{3r,k+1} \end{bmatrix}$$

$$\mathbf{B}_{1,k} = \begin{bmatrix} \Omega_{1,2,k} & \Omega_{1,3,k} & \Omega_{1,4,k} \\ 0 & \Omega_{2,2,k} & \Omega_{2,3,k} \\ 0 & \Omega_{3,2,k} & \Omega_{3,3,k} \end{bmatrix},$$

$$\mathbf{f}_{2,k} = \begin{bmatrix} w_{4,1,k}z_{1,k} + w_{4,2,k}z_{2,k} \\ w_{5,1,k}z_{3,k} + w_{5,2,k}z_{4,k} \\ w_{6,1,k}z_{5,k} + w_{6,2,k}z_{6,k} \end{bmatrix}$$

$$\mathbf{B}_{2,k} = \begin{bmatrix} \Omega_{4,3,k} & 0 & 0 \\ 0 & \Omega_{5,3,k} & 0 \\ 0 & 0 & \Omega_{6,3,k} \end{bmatrix} \quad \mathbf{u}_{1,k} = \begin{bmatrix} u_{1,k} \\ u_{2,k} \\ u_{3,k} \end{bmatrix},$$

where control matrices $\mathbf{B}_{1,k}$ and $\mathbf{B}_{2,k}$ must have full rank. Defining the first rotational block as

$$\mathbf{z}_{1,k} = \mathbf{x}_{1,k} = \begin{bmatrix} \bar{z}_{1,k} & \bar{z}_{2,k} & \bar{z}_{3,k} \end{bmatrix}^T, \tag{9}$$

taking one step ahead $\mathbf{z}_{1,k+1} = \mathbf{x}_{1,k+1} = \mathbf{f}_{1,k} + \mathbf{B}_{1,k}\mathbf{x}_{2,k}$.

Thus, assuming $\mathbf{x}_{2,k}$ as a pseudo control required to drive the error $\mathbf{z}_{1,k}$ to zero, for the expression (10)

$$\mathbf{z}_{1,k+1} = \mathbf{f}_{1,k} + \mathbf{B}_{1,k}\mathbf{x}_{2,k} = \mathbf{K}_1\mathbf{z}_{1,k}, \tag{10}$$

the following control law is derived

$$\mathbf{x}_{2r,k} = [\mathbf{B}_{1,k}]^{-1}\left[-\mathbf{f}_{1,k} + \mathbf{K}_1\mathbf{z}_{1,k}\right],$$

where $\mathbf{K}_1$ is a *Schur* diagonal matrix to guarantee convergence of $\mathbf{z}_{1,k}$ to zero. Therefore, with $\mathbf{x}_{2,k} = \mathbf{x}_{2r,k}$ the second error vector is established as

$$\mathbf{z}_{2,k} = \begin{bmatrix} \bar{z}_{4,k} & \bar{z}_{5,k} & \bar{z}_{6,k} \end{bmatrix}^T = \mathbf{x}_{2,k} - \mathbf{x}_{2r,k}. \tag{11}$$

Thus, replacing (11) in (10), one obtains

$$\mathbf{z}_{1,k+1} = \mathbf{K}_1\mathbf{z}_{1,k} + \mathbf{B}_{1,k}\mathbf{z}_{2,k}, \tag{12}$$

and from (11) the error dynamic can be obtained as

$$\mathbf{z}_{2,k+1} = \mathbf{x}_{2,k+1} - \mathbf{x}_{2r,k+1} = \mathbf{f}_{2,k} + \mathbf{B}_{2,k}\mathbf{u}_{1,k} - \mathbf{x}_{2r,k+1}$$

with $\mathbf{x}_{2r,k+1} = [\mathbf{B}_{1,k+1}]^{-1}\left[-\mathbf{f}_{1,k+1} + \mathbf{K}_1\mathbf{z}_{1,k+1}\right]$. A simplified form of the second rotational block (Block B) in the new coordinates is obtained as

$$\mathbf{z}_{2,k+1} = \tilde{\mathbf{f}}_{2,k} + \mathbf{B}_{2,k}\mathbf{u}_{1,k}, \tag{13}$$

with $\tilde{\mathbf{f}}_{2,k} = \mathbf{f}_{2,k} - \mathbf{x}_{2r,k+1}$. So, the block controllable form for the rotational motion of the system is expressed through (12) and (13).

Translational blocks: Similar to the rotational blocks, from (6) the variables of the first translational block (Block C) are defined as

$$\mathbf{x}_{3,k} = \begin{bmatrix} \hat{x}_{7,k} - x_{7r,k} \\ \hat{x}_{8,k} - x_{8r,k} \\ \hat{x}_{9,k} - x_{9r,k} \end{bmatrix}, \quad \mathbf{x}_{4,k} = \begin{bmatrix} \hat{x}_{10,k} \\ \hat{x}_{11,k} \\ \hat{x}_{12,k} \end{bmatrix},$$

so that the state estimation is expressed in the block control form as

$$\mathbf{x}_{3,k+1} = \mathbf{f}_{3,k}(\mathbf{x}_{3,k}, \hat{\mathbf{w}}_k) + \mathbf{B}_{3,k}\mathbf{x}_{4,k}, \tag{14}$$

$$\mathbf{x}_{4,k+1} = \mathbf{f}_{4,k}(\mathbf{x}_{1,k}, \mathbf{x}_{2,k}, \mathbf{x}_{4,k}, \hat{\mathbf{w}}_k) + \mathbf{B}_{4,k}\mathbf{u}_{2,k}, \tag{15}$$

with

$$\mathbf{f}_{3,k} = \begin{bmatrix} \Omega_{7,1,k} - x_{7r,k+1} \\ \Omega_{8,1,k} - x_{8r,k+1} \\ \Omega_{9,1,k} - x_{9r,k+1} \end{bmatrix}$$

$$\mathbf{B}_{3,k} = \begin{bmatrix} \Omega_{7,2,k} & (\Omega_{7,3,k} + \Omega_{7,4,k}) & (\Omega_{7,5,k} + \Omega_{7,6,k}) \\ \Omega_{8,2,k} & (\Omega_{8,3,k} + \Omega_{8,4,k}) & (\Omega_{8,5,k} + \Omega_{8,6,k}) \\ \Omega_{9,2,k} & \Omega_{9,3,k} & \Omega_{9,4,k} \end{bmatrix},$$

$$\mathbf{f}_{4,k} = \begin{bmatrix} \Omega_{10,1,k} + \cdots + \Omega_{10,4,k} + w_{10,5,k}z_{7,k} \\ \Omega_{11,1,k} + \cdots + \Omega_{11,4,k} + w_{11,5,k}z_{8,k} \\ \Omega_{12,1,k} + \cdots + \Omega_{12,4,k} + w_{12,5,k}z_{9,k} \end{bmatrix}$$

$$\mathbf{B}_{4,k} = \begin{bmatrix} 0 & 0 & 0 \\ 0 & 0 & 0 \\ 0 & 0 & \Omega_{12,6,k} \end{bmatrix} \quad \mathbf{u}_{2,k} = \begin{bmatrix} 0 \\ 0 \\ u_{4,k} \end{bmatrix},$$

where control matrices $\mathbf{B}_{3,k}$ and $\mathbf{B}_{4,k}$ must have full rank and rank-one, respectively. Defining the first translational block as

$$\mathbf{z}_{3,k} = \mathbf{x}_{3,k} = \begin{bmatrix} \bar{z}_{7,k} & \bar{z}_{8,k} & \bar{z}_{9,k} \end{bmatrix}^T, \tag{16}$$

and assuming $\mathbf{x}_{4,k}$ as a pseudo control required to drive the error $\mathbf{z}_{3,k}$ to zero, the expression (17)

$$\mathbf{z}_{3,k+1} = \mathbf{f}_{3,k} + \mathbf{B}_{3,k}\mathbf{x}_{4,k} = \mathbf{K}_2\mathbf{z}_{3,k}, \tag{17}$$

the following control law is derived

$$\mathbf{x}_{4r,k} = [\mathbf{B}_{3,k}]^{-1}\left[-\mathbf{f}_{3,k} + \mathbf{K}_2\mathbf{z}_{3,k}\right],$$

where $\mathbf{K}_2$ is a *Schur* diagonal matrix. Therefore, to set $\mathbf{x}_{4,k} = \mathbf{x}_{4r,k}$ the second error vector is established as

$$\mathbf{z}_{4,k} = \begin{bmatrix} \bar{z}_{10,k} & \bar{z}_{11,k} & \bar{z}_{12,k} \end{bmatrix}^T = \mathbf{x}_{4,k} - \mathbf{x}_{4r,k}. \tag{18}$$

Thus, replacing (18) in (17) one obtains

$$\mathbf{z}_{3,k+1} = \mathbf{K}_2\mathbf{z}_{3,k} + \mathbf{B}_{3,k}\mathbf{z}_{4,k}, \tag{19}$$

and from (18) the error dynamics can be obtained as

$$\mathbf{z}_{4,k+1} = \mathbf{x}_{4,k+1} - \mathbf{x}_{4r,k+1} = \mathbf{f}_{4,k} + \mathbf{B}_{4,k}\mathbf{u}_{2,k} - \mathbf{x}_{4r,k+1}$$

with $\mathbf{x}_{4r,k+1} = [\mathbf{B}_{3,k+1}]^{-1}[-\mathbf{f}_{3,k+1} + \mathbf{K}_2\mathbf{z}_{3,k+1}]$. In this way, a simplified form of the second rotational block (Block D) in new coordinates is obtained as

$$\mathbf{z}_{4,k+1} = \tilde{\mathbf{f}}_{4,k} + \mathbf{B}_{4,k}\mathbf{u}_{2,k}, \tag{20}$$

with $\tilde{\mathbf{f}}_{4,k} = \mathbf{f}_{4,k} - \mathbf{x}_{4r,k+1}$. Finally, the block controllable form for the translational motion is expressed through the equations (19) and (20).

C. Discrete-Time Sliding Mode Control

For the rotational case, assuming $\mathbf{u}_{1,k} = \mathbf{B}_{2,k}^{-1}\mathbf{v}_{1,k}$, and using block controllable form established by (12) and (13), the sliding manifold vector is defined as $\mathbf{S}_{1,k} = \mathbf{z}_{2,k} = 0$. Taking one step ahead and using (13), the rotational dynamics of the system is transformed into

$$\begin{aligned} \mathbf{z}_{1,k+1} &= \mathbf{K}_1\mathbf{z}_{1,k} + \mathbf{B}_{1,k}\mathbf{z}_{2,k}, \\ \mathbf{S}_{1,k+1} &= \tilde{\mathbf{f}}_{2,k} + \mathbf{v}_{1,k}, \end{aligned} \tag{21}$$

where equivalent control $\mathbf{v}_{1,eq,k}$ that satisfies $\mathbf{S}_{1,k+1} = 0$ corresponds to $\mathbf{v}_{1eq,k} = -\tilde{\mathbf{f}}_{2,k}$. In this way, a discrete-time sliding mode control law is proposed as

$$\mathbf{v}_{1,k} = \left\{ \begin{array}{lll} \mathbf{v}_{1eq,k}, & \text{for} & \|\mathbf{v}_{1eq,k}\| \leq \mathbf{v}_{1,0} \\ \mathbf{v}_{1,0}\frac{\mathbf{v}_{1eq,k}}{\|\mathbf{v}_{1eq,k}\|}, & \text{for} & \|\mathbf{v}_{1eq,k}\| > \mathbf{v}_{1,0} \end{array} \right\} \tag{22}$$

where $\mathbf{v}_{1,0}$ corresponds to the controller saturation limit

On the other hand, for the translational case, assuming $\mathbf{u}_{2,k} = \bar{\mathbf{B}}_{4,k}\mathbf{v}_{2,k}$ where $\bar{\mathbf{B}}_{4,k}$ is the pseudo inverse matrix of $\mathbf{B}_{4,k}$, and using the block controllable form defined in (19) and (20), the sliding manifold vector is defined as $\mathbf{S}_{2,k} = \mathbf{z}_{4,k} = 0$, where equivalent control $\mathbf{v}_{2,eq,k}$ that satisfies $\mathbf{S}_{2,k+1} = 0$ corresponds to $\mathbf{v}_{2eq,k} = -\tilde{\mathbf{f}}_{4,k}$, such that, a discrete-time sliding mode control law corresponds to

$$\mathbf{v}_{2,k} = \left\{ \begin{array}{lll} \mathbf{v}_{2eq,k}, & \text{for} & \|\mathbf{v}_{2eq,k}\| \leq \mathbf{v}_{2,0} \\ \mathbf{v}_{2,0}\frac{\mathbf{v}_{2eq,k}}{\|\mathbf{v}_{2eq,k}\|}, & \text{for} & \|\mathbf{v}_{2eq,k}\| > \mathbf{v}_{2,0} \end{array} \right\} \tag{23}$$

where $\mathbf{v}_{2,0}$ is the controller saturation [8].

IV. SIMULATIONS

The parameters used for simulation correspond to a real Quanser Qball-X4 prototype (Table. II). To illustrate the effectiveness of the discrete-time proposed control scheme for trajectory tracking, it is considered to follow a trajectory generated by a Rossler-type chaotic attractor in discrete-time, changing its orientation at a rate of $5\,[^\circ/s]$, with an instantaneous mass change corresponding to $25\,[\%]$ of the quadrotor total mass at $t = 400\,[s]$ and $t = 1200\,[s]$. In this way, translational trajectory tracking can be seen in Fig. 6, and the respective orientation in Fig. 7. Additionally, Fig. 8 presents the thrust required in the propellers, where a considerable change in the thrusts can be observed when the quadrotor gains and loses mass. To show the behavior

TABLE II: System parameters

Symbol	Quantity	Value
I_1	Moment of inertia around the b_1 axis	$0.03\ [kg \cdot m^2]$
I_2	Moment of inertia around the b_2 axis	$0.03\ [kg \cdot m^2]$
I_3	Moment of inertia around the b_3 axis	$0.04\ [kg \cdot m^2]$
m_G	Total moving mass of the quadrotor	$1.4\ [kg]$
T_λ	Maximum thrust of the λ-th propeller	$15\,[N]$
κ_S	Useful thrust ratio in yaw rotation	$0.1\,[m]$
L	Horizontal distance between the center of mass and each propeller	$0.2\,[m]$
d	Vertical distance between the center of mass and each propeller	$0.02\,[m]$
g	Force of gravity	$10\ [m/s^2]$
T_s	Sampling time	$0.02\,[s]$

of the controlled system under the effect of non-vanishing disturbances typical of an flight uncontrolled environment, a circular track is selected for this experiment. Thus, Fig. 9 shows the behavior of the system when a turbulent and random wind, presented in in Fig. 10, hits the blades of each propeller at a flap angle $\alpha_\lambda = 5\,[^\circ]$, at the same time that a wind as in Fig. 11, drags the quadrotor from its center of mass m_G, driving it out of its desired track.

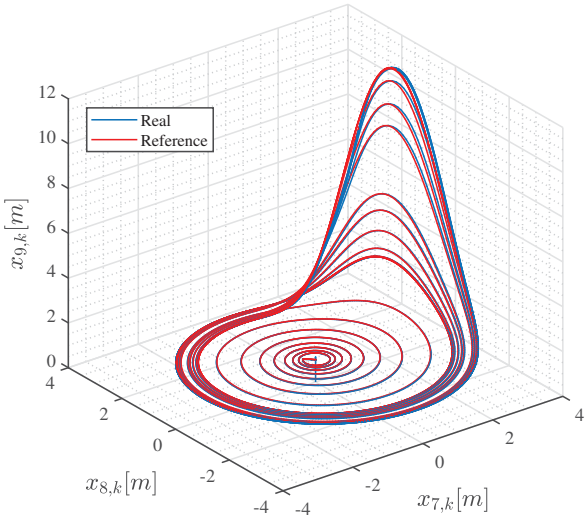

Fig. 6: 3D view - Rossler-type chaotic attractor

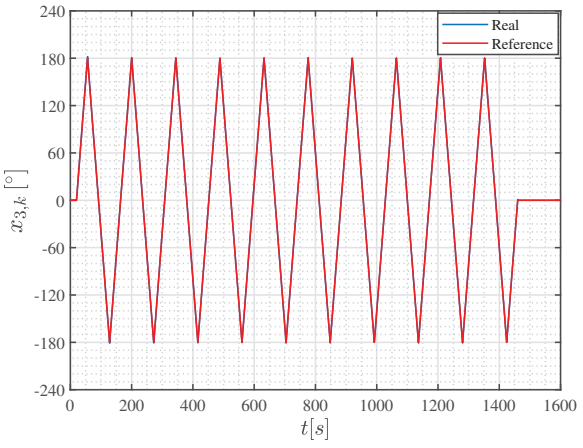

Fig. 7: Orientation change in ψ_k

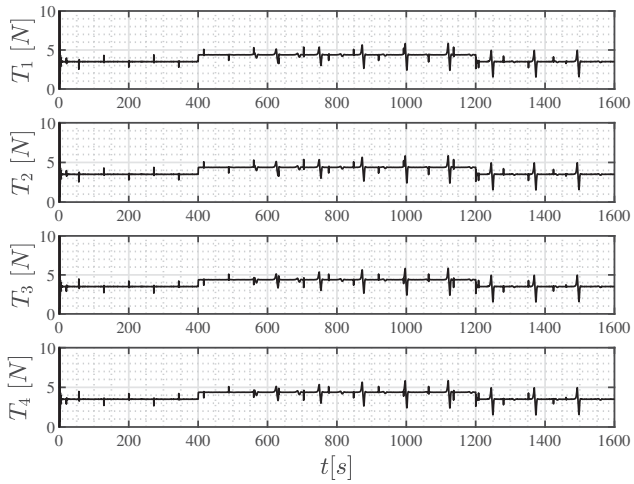

Fig. 8: Applied thrusts

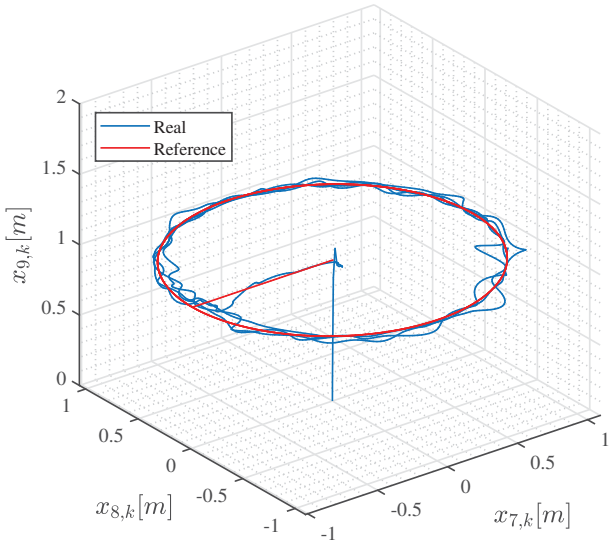

Fig. 9: 3D view - Disturbed circle by wind

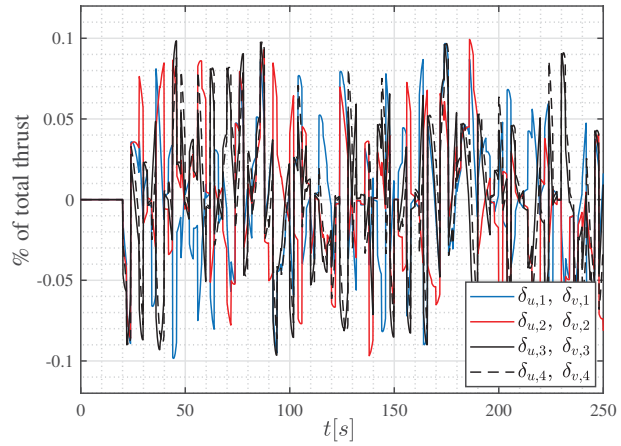

Fig. 10: Blade flapping in rotors

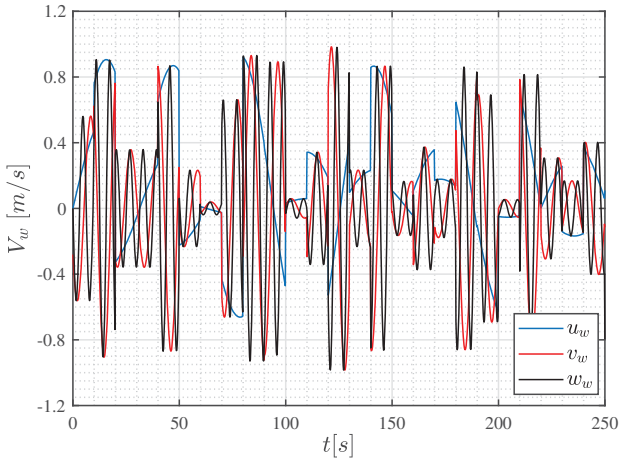

Fig. 11: Wind velocity in the body

V. CONCLUSIONS

The obtained mathematical model of the quadrotor is highlighted. From the results, the ability of the model to simultaneously change its position and orientation is observed. Also, it is evident the ability of the proposed controller based on a neuronal identifier to guarantee tracking of the quadrotor trajectory, even in presence of unknown non-vanishing perturbations, such that, incident wind and change of mass. Regarding the latter, it is concluded that the change in the thrust magnitude shown in Fig. 8 is directly proportional to the transported mass.

REFERENCES

[1] J. Craig. *Introduction to Robotics: Mechanics and Control*. Pearson Education, 2005.

[2] J. G. Leishman. *Principles of Helicopter Aerodynamics*. Cambridge University Press, The Edinburgh Building, Cambridge CB2 2RU, UK. 2000.

[3] G. Hoffmann, H. Huang, S. Waslander, and C. Tomlin, "Quadrotor helicopter flight dynamics and control: Theory and experiment," AIAA guidance, navigation and control conference and exhibit, 2007.

[4] M. Norgaard, O. Ravn, N. K. Poulsen, and L. K. Hansen, "Neural networks for modelling and control of dynamic systems: a practitioner's handbook," Advanced textbooks in control and signal processing, Springer, Berlin, 2000.

[5] E. N. Sanchez, A. Y. Alanís, and A. G. Loukianov. *Discrete-Time High Order Neural Control: Trained with Kalman Filtering*. Springer Science & Business Media, 2008, vol. 112.

[6] G. A. Rovithakis and M. A. Christodoulou, "Adaptive control with recurrent high-order neural networks: theory and industrial applications," Springer Science & Business Media, 2012.

[7] V. I. Utkin, "Sliding mode control in discrete-time and difference systems," Springer Berlin Heidelberg, Berlin, Heidelberg, 1994, pp. 87–107.

[8] V. Utkin, J. Guldner, and J. Shi. *Sliding Mode Control in Electro-Mechanical Systems*. CRC Press, 2009.

[9] F. Ornelas-Tellez, E. N. Sanchez, and A. G. Loukianov, "Discrete-time inverse optimal control for block control form nonlinear systems," World Automation Congress 2012. IEEE, 2012.